

Creep Behavior of Biaxial Cold-Rolled Polypropylene

J. X. LI and W. L. CHEUNG*

Department of Mechanical Engineering, University of Hong Kong, Pokfulam Road, Hong Kong

SYNOPSIS

Polypropylene was biaxially rolled up to 60% at ambient temperature, and the tensile creep behavior over the temperature range 27 to 60°C was investigated using a dead-load apparatus. The degrees of crystallinity of the as-molded and rolled PP were determined using a differential scanning calorimeter (DSC) and density bottle. The DSC showed a slight change in the crystallinity during the early stage of the rolling process, while the density bottle indicated a continuous drop of the density with increasing rolling reduction. The elongation due to rolling was found almost fully recoverable when the samples were thrown into hot silicon oil at 180°C. The effects of cold rolling on creep strain, secondary creep strain rate, and creep activation energy were investigated. Cold rolling led to an increase in the creep strain and secondary creep strain rate. The creep activation energy was found to increase with increasing rolling reduction. Within the secondary creep stage, the creep process in polypropylene is mainly due to the α -relaxation process and most of the creep strain was recoverable. © 1995 John Wiley & Sons, Inc.

INTRODUCTION

Cold rolling is a well-known means of improving the mechanical properties, such as tensile strength and hardness, of metallic materials. In the past 3 decades, this manufacturing process has also attracted interest of many polymer researchers. Gruenwald¹ reported the effect of cold rolling on polycarbonate. Rothschild and Maxwell² studied the changes in tensile properties of polyethylene after uniaxial rolling up to 50% and came to the following conclusions. Cold rolling increases the tensile strength and slightly decreases the ultimate elongation in the rolling direction. Maximum strength perpendicular to the rolling direction is reduced but the ultimate elongation is increased.

Wilchinsky³ examined the crystal orientation of cold-rolled polypropylene using x-ray diffraction techniques and observed a bimodal distribution of the crystallite *c* axis symmetrical about the rolling direction. Dhingra et al.⁴ extended the study of morphological structure to cross-rolled polypropylene and observed a planar type orientation with the chain axes parallel to the rolling surface.

Cold rolling was also shown to reduce the brittleness temperature of polypropylene.⁵ Litt and Koch⁶ reported the effect of internal stress due to cold rolling on the cold flow of glassy polymers. Peterlin⁷ found that cold rolling of high density polyethylene increases the elastic modulus and ultimate strength, reaching an asymptotic value beyond a draw ratio of 20. Broutman and co-workers⁸⁻¹⁰ studied the effects of cold rolling on the drawability, tensile properties, and impact strength of a number of amorphous polymers, such as polycarbonate, polysulphones, polyphenylene oxides, and acrylonitrile-butadiene-styrenes. Bahadur and Henkin¹¹ studied the effect of cold rolling on the mechanical properties of acetal, nylon 66, poly(vinyl chloride) and polycarbonate. They concluded that the changes in the properties are not due to the unique loading or heating and cooling cycle involved in the rolling process but to the morphological changes produced in the polymers. Kitagawa et al.¹² studied the crack growth under static and fatigue loading in glassy polymers oriented by cold rolling. Lee and Kung¹³ studied the elimination of stress whitening in high-molecular weight polyethylene after cold rolling. They concluded that at 40% or more rolling reduction the macro- and microimperfections were largely eliminated; hence, stress whitening did not occur.

* To whom correspondence should be addressed.

Although considerable attention has been focused on the tensile properties and manufacturing behavior of cold-rolled plastics, little effort has been directed toward the long-term creep behavior. In this study, the creep and recovery behavior of the unrolled and rolled PP was investigated. The melt flow index (MFI), density, and crystallinity of the unrolled and rolled PP were also determined in order to assess the effect of cold rolling on the molecular and morphological structure of the polymer.

EXPERIMENTAL

Materials and Processing

The isotactic polypropylene used in this study was Shell KM6100 in granule form. The polymer was compression molded into square pads of different thicknesses ranging from 1.5 to 4.0 mm. The PP granule in a stainless steel mold was first heated at 200°C between the hot platens of the molding press under slight pressure. After 3 min, the clamping force on the mold was gradually increased to 10 tonnes. The mold was then removed from the press and immediately quenched in water at room temperature.

Apart from the 1.5 mm thick pads, all other pads were crossrolled at room temperature in a rolling mill with 90 mm diameter rolls operating at 42 rpm. In every pass, the thickness of the pad was reduced by about 0.05 mm. The pad was then turned 90° to the previous rolling direction for the next pass. This procedure was repeated until the required rolling reduction was achieved. The nominal final thickness of the rolled pads was 1.8 mm. The required rolling reduction was attained by choosing an appropriate starting thickness, which was then rolled to 1.8 mm.

An annealing process was adopted to flatten the rolled PP pads. Both the rolled and unrolled pads were annealed at 60°C for 12 h. No obvious thickness change was observed after the annealing process. The pads were then cut into dumbbell-shaped specimens with gauge length 80 mm and width 12 mm.

Creep Tests

The creep tests were performed in a Ceast 6110/000 creep tester equipped with a digital data acquisition system. Five specimens can be tested simultaneously at a set temperature. The specimens were conditioned at the testing temperature before application of load. The creep elongations were measured using linear voltage-displacement transducers. The output

signals from the transducers were digitized and fed into a computer for further processing.

In order to avoid slippage of the specimens in the self-fixed grips upon application of load, preliminary loading was applied on the specimens for about 1 min. The load was removed and the specimens were allowed to recover for 10 min. The displacement registered by the transducer was noted. The preliminary loading procedure was repeated until the displacement upon removal of load became repeatable and then the transducers were readjusted to zero. All the tests were performed under a load equivalent to an initial stress of 8 MPa. The testing temperature varied from room temperature (27°C) to 60°C.

Crystallinity and Melt Flow Index Measurement

Differential scanning calorimeter (DSC) and density bottle were used to determine the crystallinity of the rolled and unrolled PP. In the former method, a DuPont 910 DSC was used to measure the fusion heat of the samples. The degree of crystallinity was determined by comparing the average fusion heat of three samples with that of 100% crystalline PP. The value 170 J/g was adopted as the fusion heat of 100% crystalline PP.¹⁴ The heating rate was 5°C/min, and a stream of nitrogen, 5 mL/min, was used as the purging gas during the DSC tests. In the density bottle method, the relative densities of 100% crystalline and amorphous PP were taken as 0.936 and 0.852, respectively.¹⁵ The melt flow indexes of the PP samples were measured using a Davenport Melt Indexer that operated at 190°C with a 2160 g load.

Molecular Coil Extension Ration Measurement

Rectangular strips, 8 mm wide and 80 mm long, were cut from the rolled PP pads along the rolling directions. They were thrown into a silicon oil bath in an oven at 180°C for 3 min. The silicon oil bath was then removed from the oven and allowed to cool to room temperature. The molecular coil extension ratio due to rolling was defined as the original length of the strip, i.e., 80 mm, over that after the silicon oil bath treatment.

RESULTS AND DISCUSSION

Crystallinity, Melt Flow Index and Molecular Coil Extension Ratio

Figure 1 shows the effect of rolling reduction on the crystallinity of the samples obtained by DSC and

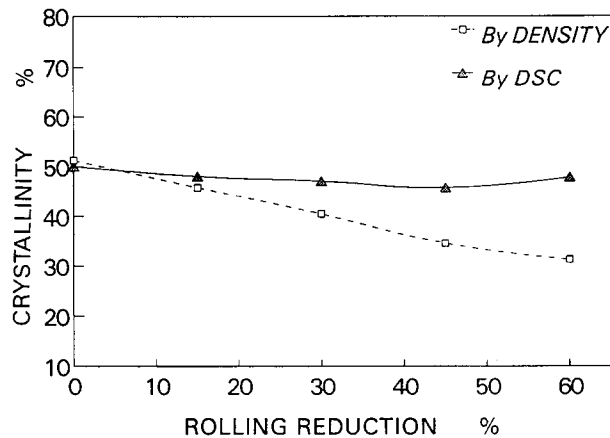


Figure 1 Effect of rolling reduction on crystallinity.

density bottle. Both methods suggest that the unrolled PP has a crystallinity of about 50%. The crystallinity by DSC drops to about 48% as the rolling reduction is increased to 15%. When the rolling reduction is further increased from 15 to 60%, however, there is little change in the crystallinity and the curve waves around 47%. In contrast, the crystallinity based on density drops continuously to about 32% as the rolling reduction is increased to 60%. It was later found by scanning electron microscopy that voids existed in the cold-rolled samples. Thus, density bottle is not a good method for studying the change of crystallinity because it is affected by voids formed during rolling.

In Dhingra's study,⁴ the crystallinity of rolled PP decreased rapidly from 60 to 48% when the rolling reduction was increased from 0 to 30%, then the crystallinity waved around 48% with further increase in rolling reduction. Although the crystallinity did not drop greatly in this study during early stage of the rolling process, the trend of decreasing and then leveling off was similar. The above observations seem to indicate that the effect of rolling on crystallinity depends not only on the reduction ratio but also the initial crystallinity of PP. The initial crystallinity of our molded samples was about 50%, which was 10% lower than those of Dhingra's. This might be the reason why we only observed a drop of about 2% in crystallinity during early stage of our rolling process.

The stretch ratios along the rolling directions were calculated assuming no volume change in the material, and are listed in Table I together with the melt flow index and the molecular coil extension ratio by abrupt fusion in hot silicon oil. The values of the molecular coil extension ratio and the calculated stretch ratio are very close, indicating that

most of the deformation is recoverable by the abrupt fusion process. However, it should be noticed that the molecular coil extension ratio is smaller than the calculated stretch ratio in all the rolled samples. In other words, the rolled PP never fully recovered. The difference between the two quantities also suggests that the amount of nonrecoverable deformation increases with increasing rolling reduction. At low rolling reduction, deformation is mainly in the amorphous material because of its lower modulus, while the crystals are relatively unaffected. At high rolling reduction, disintegration of crystals and voiding may occur; also, some molecular chains may break due to excessive strain. This is in agreement with the results of the melt flow index (MFI) tests. The PP granule has a MFI of 1.55 and that of the unrolled PP was 1.56, virtually unchanged after the compression molding process. It increased gradually to 1.64 as the PP was rolled to 60%. It is believed that some molecules were broken during the rolling process, resulting in a drop of the molecular weight and, thus, the MFI decreased.

Creep Behavior

A typical creep curve of the rolled PP is shown in Figure 2. In the primary creep stage, OA, the creep strain increases rapidly, whereas the creep strain rate decreases. In the secondary creep stage, the creep strain rate approaches to a constant value and the creep process is said to be in steady state. Beyond this region, necking and cavitation in specimens may occur and dimension of the cross-section changes greatly; thus, accurate stress analysis becomes difficult. So in this study, the creep tests were performed within the secondary stage.

When the load was removed at point B, an immediate elastic recovery occurred followed by a gradual recovery. The strain reduced to a constant value after a sufficiently long period. This remnant strain appeared to be permanent at the creep tem-

Table I Variation of MFI, Stretch Ratio and Molecular Coil Extension Ratio with Rolling Reduction

Rolling Reduction (%)	0	15	30	45	60
Melt flow index (g/10 min)	1.56	1.59	1.60	1.58	1.64
Stretch ratio	1	1.08	1.19	1.35	1.58
Molecular coil extension ratio	1	1.05	1.14	1.23	1.38

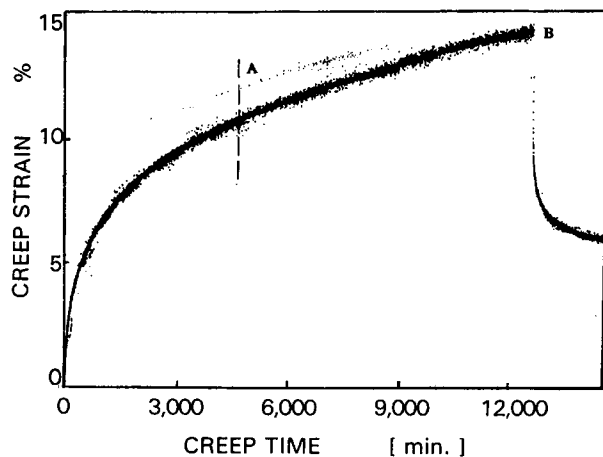


Figure 2 A typical creep curve of the rolled PP, rolling reduction 30%, and testing temperature 50°C. The data away from the main track are due to fluctuation of voltage input to the LVDT.

perature. However, when the specimens were annealed at an elevated temperature, it would reduce further. The remnant strains after free recovery at the creep temperature and elevated temperature recovery are listed in Table II. For the specimens tested at 27°C for 720 h, the remnant strain after free recovery increased from 0.4% for the unrolled samples to 2.5% for the samples with 60% rolling reduction. After the specimens had been annealed at 60°C for 6 h, however, the remnant strain in most samples reduced to zero and the maximum remnant strain was only 0.3%. For specimens tested at 60°C for 125 h, though, a 9.5% remnant strain still existed in the specimen with 30% rolling reduction after free recovery, only 1.3% strain remained after annealing at 100°C for 4 h. Furthermore, for specimens with 60% or higher rolling reductions, the strain even became negative after annealing. Obviously, this was due to relaxation of the extended molecular chain coils formed during rolling.

When the tested and annealed specimens were thrown into hot silicon oil at 180°C, their gauge lengths would reduce. Table III shows the gauge lengths of the tested samples after annealing and abrupt fusion in the silicon oil bath, together with the gauge lengths of the as-rolled samples after the abrupt fusion. It can be seen that the maximum difference between the tested and as-rolled samples after the abrupt fusion is less than 1.5 mm. This indicates that the true permanent deformation was very small, and most of the creep strain was recoverable.

Figure 3(a-d) shows the effect of temperature on the creep strain-time plots. As expected, the creep

strain increases with increasing temperature for all the rolled and unrolled samples. Nevertheless, it should be noticed that the creep strain increases more rapidly for specimens with higher rolling reduction.

Figure 4(a-d) shows the effect of rolling reduction on the creep strain-log time plots obtained at 27, 40, 50, and 60°C, respectively. It is clear that the creep strain increases with rolling reduction in all four cases. It is generally recognized that an increase in molecular orientation along the testing direction would result in reduction in creep strain. Indeed, Duxbury and Ward¹⁶ observed a reduction in the creep strain of ultrahigh modulus PP, which was drawn to draw ratios in the range 10 to 17.5. Cakmak and Wang¹⁷ observed similar reduction in the creep response for biaxial oriented PET films with stretch ratios 2 × 2 and 3 × 3.

Our results appear to be contradicting with theirs. The structure of the high-modulus PP prepared by Duxbury and Ward should be highly fibrous after suffering from such draw ratios. In this study, the maximum stretch ratio corresponding to 60% rolling reduction was about 1.6 × 1.6, which was similar to that of Cakmak and Wang. However the crystallinity of their stretched PET films increased with creasing stretch ratio, and it is difficult to isolate the purely orientational effect. Whereas the crystallinity of our rolled PP remained almost unchanged, so the change in creep behavior was likely caused by other structural changes. The above observations suggest that within the rolling reduction limit of this study the molecular orientational effect is not significant. On contrary, local yielding, voiding, and breaking of some molecular chains that occurred during rolling would speed up the creep process.

Some unrolled and rolled PP samples were melted

Table II Remnant Strains after Free Recovery and Elevated Temperature Recovery

Rolling Reduction (%)	0	15	30	60
Tested at 27°C for 720 h				
Creep strain (%)	2.4	3.2	4.5	6.8
Free recovery (%)	0.4	1.3	1.8	2.5
Recovery at 60°C for 6 h (%)				
	0	0.3	0	0
Tested at 60°C for 125 h				
Creep strain (%)	5.5	8.5	14	25
Free recovery (%)	1.5	2.8	9.5	19
Recovery at 100°C for 4 h (%)				
	0.6	0.6	1.3	-4.4

Table III Variation of Gauge Length after Different Heat Treatments, Original Gauge Length 80 mm

Rolling Reduction (%)	0	15	30	45	60
Samples tested at 27°C for 125 h					
After annealed at 100°C for 4 h (mm)	80.5	80.5	81	79.5	76.5
After abrupt fusion (mm)	80	76	71	67	60
As-rolled samples					
After abrupt fusion (mm)	80	76	70	65.5	59

again under the press at 190°C and recrystallized by water quenching. Their creep behaviors were investigated, and the results are shown in Figure 5. It can be seen that there is no obvious difference in their creep responses. This indicates that the effect of rolling is removed after the melting and recrystallization process.

The creep behavior of polymers is affected by three major parameters, i.e., stress (σ), time (t), and absolute temperature (T). The total creep strain (ϵ)

is often approximated by the following empirical power law equation.¹⁷⁻¹⁹

$$\epsilon = \epsilon_o + a_o t^n \sigma^m \exp(-Q/RT)$$

where ϵ_o is the elastic deformation, a_o , n , and m are constants related to the material, Q is the activation energy, and R is the gas constant. If the elastic deformation ϵ_o can be separated from the total strain, then the time-dependent creep strain ϵ_c becomes

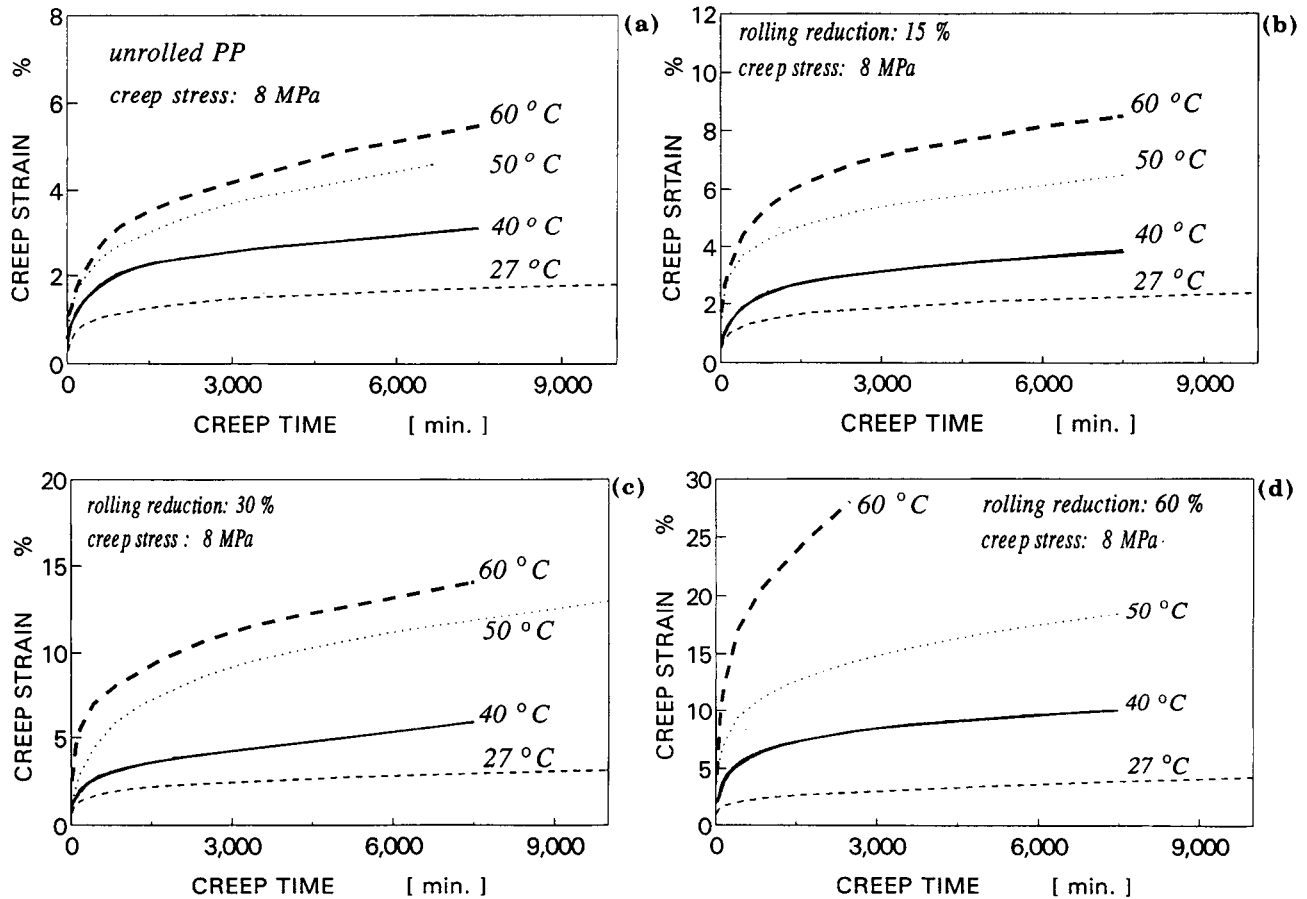


Figure 3 Effect of temperature on creep strain. (a) Unrolled PP; (b) rolling reduction 15%; (c) rolling reduction 30%; and (d) rolling reduction 60%.

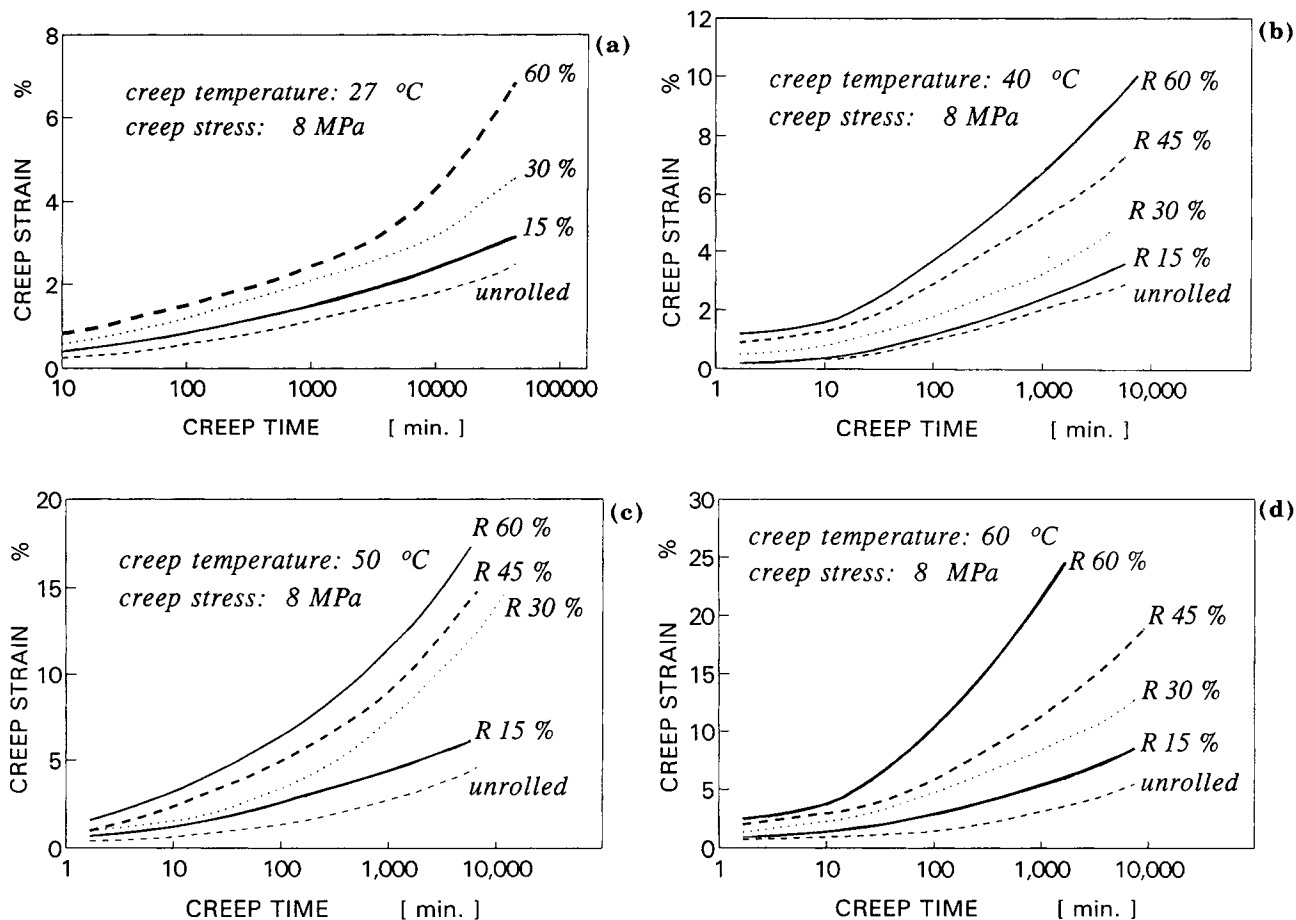


Figure 4 Creep strain-log time relations of the rolled and unrolled samples. (a) Creep temperature 27°C; (b) creep temperature 40°C; (c) creep temperature 50°C; and (d) creep temperature 60°C.

$$\epsilon_c = a_0 t^n \sigma^m \exp(-Q/RT)$$

For a particular time and stress, the activation energy Q can be obtained from the slope of the $\ln \epsilon_c$ vs. $1/T$ plot.^{17,19} However, it is not always easy to separate the elastic deformation ϵ_0 from the total strain.

Table IV Secondary Creep Strain Rates at Various Testing Temperatures, Creep Stress 8 MPa

Rolling Reduction (%)	0	15	30	60
Secondary creep strain rate (10^{-5} h)				
27°C	1.3	1.6	2.6	3.5
40°C	3.3	7.3	8.9	19.2
50°C	7.6	12.0	19.0	38.5
60°C	14.4	21.0	37.2	89.3

In the secondary creep stage, the creep strain rate is more or less constant, and a linear relationship should exist between $\ln \dot{\epsilon}$ and $1/T$ as follows:

$$\ln \dot{\epsilon}_p = -Q/RT + \text{constant}$$

where $\dot{\epsilon}_p$ is the secondary creep strain rate. Figure 6 shows the plots of $\ln \dot{\epsilon}_p$ vs. $1/T$ for samples of different rolling reductions. As expected, the plots exhibit good linearity. The activation energies were calculated from the slopes of the straight lines fitted to the experimental data using linear regression method. The results were plotted against the rolling reduction in Figure 7. For the unrolled PP, the value of Q is 15.5 kcal/mol. At 15% rolling reduction, Q is virtually unchanged at 15.4 kcal/mol and at 30% rolling reduction, Q increases slightly to 16.1 kcal/mol. However, Q increases substantially to 19.3 kcal/mol at 60% rolling reduction, showing the higher strain rate de-

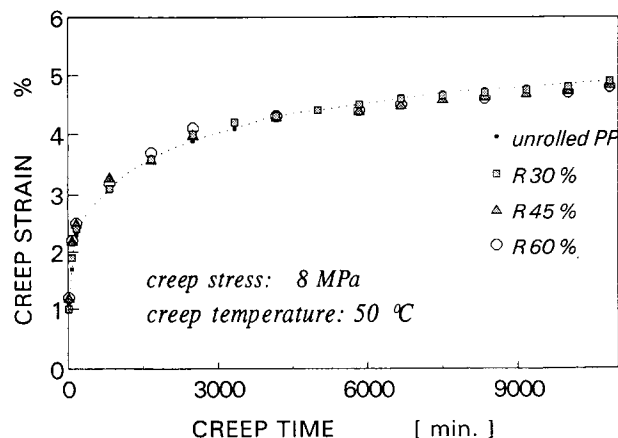


Figure 5 Creep response of the rolled and unrolled samples after melted at 190°C and then recrystallized by water quenching.

pendence on temperature of the samples. Nevertheless, the values of the activation energy are within the range for the α -relaxation process,^{20,21} which is usually attributed to the segmental motion of the main chain.

CONCLUSION

For polypropylene with 50% initial crystallinity, biaxial cold rolling led to a 2% decrease in the crystallinity at 15% rolling reduction, and for further rolling up to 60% there was little change in the crystallinity. In contrast, the density dropped continuously with increasing rolling reduction due to formation of voids in the specimens. Most of the de-

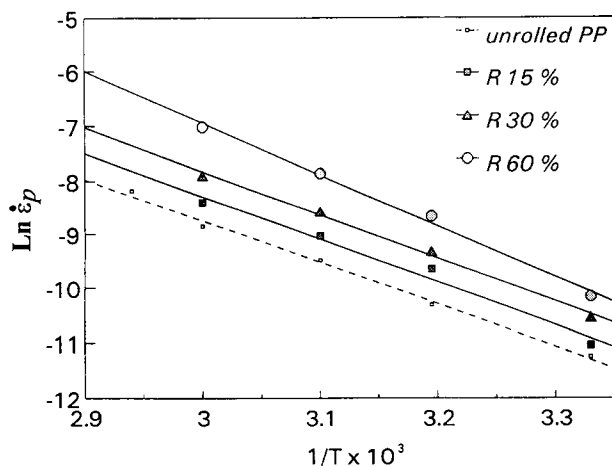


Figure 6 $\ln \dot{\epsilon}_p$ vs. $1/T$ plots for the rolled and unrolled samples. The straight lines are obtained by linear regression method.

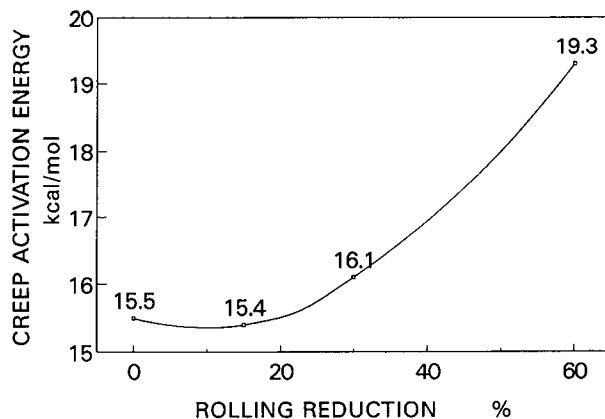


Figure 7 Effect of rolling reduction on creep activation energy.

formation due to rolling arose from extension of molecular chains that could be recovered by abrupt fusion in the silicon oil bath at 180°C. The total creep strain and the secondary creep strain rate increased with rolling reduction for the temperatures, stress, and time investigated in this study. The creep strains were mostly recovered after annealing at elevated temperatures below the melting point of the polymer. The creep activation energy was found to increase with rolling reduction, indicating that the strain rate dependence on temperature increase with rolling reduction. Within the secondary creep stage, polypropylene creeps mainly by means of the α -relaxation process.

The assistance of Mr. K. H. Lee in conducting some of the experiments is greatly acknowledged. One of us, J. X. Li, was supported on a CRCG grant during the course of this work.

REFERENCES

1. G. Gruenwald, *Modern Plastics*, **38**, 137 (1960).
2. P. H. Rothschild and B. Maxwell, *J. Appl. Polym. Sci.*, **5**, 5 (1961).
3. Z. W. Wilchinsky, *J. Appl. Polym. Sci.*, **7**, 923 (1963).
4. V. J. Dhingra, J. E. Spruil, and E. S. Clark, in *Proceedings of SPE 39th Annual Technical Conference and Exhibition (ANTEC 39)*, Boston, May 1981, p. 114.
5. Z. W. Wilchinsky, *SPE J.*, **22**, 46 March 1966.
6. M. H. Litt and P. Koch, *J. Polym. Sci.*, **5b**, 251 (1967).
7. A. Peterlin, *Kolloid*, **233**, 857 (1969).
8. L. J. Broutman and S. Kalpakjian, *SPE J.*, **25**, 46 (1969).
9. L. J. Broutman and R. S. Patil, *Polym. Eng. Sci.*, **11**(2), 165 (1971).

10. L. J. Broutman and S. M. Krishnakumar, *Polym. Eng. Sci.*, **14**(4), 249 (1974).
11. S. Bahadur and A. Hekin, *Polym. Eng. Sci.*, **13**(6), 422 (1973).
12. M. Kitagawa, S. Isobe, and H. Asano, *Polymer*, **23**, 1830 (1982).
13. Y. W. Lee and S. H. Kung, *J. Appl. Polym. Sci.*, **46**, 9 (1992).
14. I. Kirshenbaum, Z. W. Wilchinsky, and B. Groten, *J. Appl. Polym. Sci.*, **8**, 2723 (1964).
15. J. Brandrup and E. H. Immergut, *Polym. Handbook*, V23 (1975).
16. J. Duxbury and I. M. Ward, *J. Mater. Sci.*, **22**, 1215 (1987).
17. M. Cakmak and Y. D. Wang, *J. Appl. Polym. Eng. Sci.*, **41**, 1867 (1990).
18. W. N. Findley and J. F. Tracy, *Polym. Eng. Sci.*, **14**, 577 (1974).
19. G. G. Trantina, *Polym. Eng. Sci.*, **26**(11), 776 (1986).
20. J. V. Dawkins, *Development in Polymer Characterisation*, Applied Science Publisher, London, 1983, pp. 155-183.
21. J. L. Koenig, *Probing Polymer Structure*, American Chemical Society, Washington, DC, 1979, p. 218.

Received October 25, 1993

Accepted September 9, 1994